Investigation of Structural, Thermal Properties and Shielding Parameters of Borosilicate Glasses Doped with Dy^{3+}/ Tb^{3+} Ions for Gamma and Neutron Radiation Shielding Applications

Bashar Khudhair Abbas[1,*], Sharudin Omar Baki[2,♣], Fong Wai Leng[1], Haider Khudhair Abbas[3], Layth Al-Sarraj[4], Mohd Adzir Mahdi[1]

[1] Wireless and Photonic Networks Research Centre, Faculty of Engineering, Universiti Putra Malaysia, 43400 Serdang, Selangor, Malaysia
[2] Physics Division, Centre of Foundation Studies for Agricultural Science, Universiti Putra Malaysia, 43400 Serdang, Selangor, Malaysia
[3] Research Centre of IT Technology, Ministry of Electricity, Baghdad, Iraq
[4] IT Dep./ Prospect Vision Engineering Company, Baghdad, Iraq

ARTICLE INFO	ABSTRACT
	In this study, borosilicate host (H) and seven (S1-S7) samples are prepared by traditional melt-quenching technique. The samples are singly (S1, S2) and doubly (S3-S7) doped with deferent contents of Tb^{3+} and Dy^{3+} ions. All samples are analyzed and characterized by XRD (x-ray diffraction), ATR-FTIR (Attenuated total Reflectance-Fourier transform infrared) spectroscopy, TGA/DSC (Thermogravimetric analysis/Differential scanning calorimetry), and Raman spectroscopy. Moreover, the radiation shielding parameters of mentioned glasses such as mass attenuation (μ/ρ), mean free path (MFP), and half-value layer (HVL) are evaluated within the energy of 0.015MeV-15MeV. These parameters are theoretically investigated and evaluated by using XCOM, WINXCOM, and Phy-X programs in addition to the other relevant equations. The ATR-FTIR measurement and Raman spectroscopy results confirmed the unit structure of BO_3 and BO_4 groups as the main compound as well as the Aluminum-oxide (Al-O-Al) and zinc-oxide (ZnO_4) bonds. The transition (T_g), onset crystallization (T_x), crystallization (T_c) temperatures, and weight loss were identified from DSC and TGA findings, respectively. Also, the prepared glass shows good stability against crystallization, as reflected by (ΔT) variation. Furthermore, the radiation shielding parameter findings show good enhancement of the performance of the samples. However, upon these findings, one can say that these glasses could be used and utilized for radiation shielding purposes.

---

* Corresponding author.
E-mail address: basharabbass8@gmail.com

♣ Corresponding author.
E-mail address: sharudinomar@upm.edu.my

1. Introduction

Recently, borosilicate glasses attract the researcher's attention due to their properties and performance in various applications. Also, there is more interest in developing good radiation shielding materials against gamma rays and neutrons [1-3]. Currently, the concretes are using for protection from radiation as shielding materials were they are cost-effective, and their shapes and sizes are easily controllable [4]. At the same time, concretes have many disadvantages like decrement in density, cracks formation, chemical damage and not transparency, etc.[5]. Thus, glass as shielding material against radiations like gamma-rays being a choice to be instead of concretes where the glasses are transparent. However, due to the toxic effects of Pb-based glasses, numerous studies have been done to replace it with tellurite [6], borate [7], silicate [8], boro-tellurite [9] and borosilicate [10].

To get a vision about the interaction of radiation with shielding materials, some essential parameters must be considered and evaluated such as the mass attenuation coefficient (μ/ρ), half-value layer (HVL), effective atomic number (Z_{eff}), and mean free path (MFP). In fact, the low quantity of the MFP and HVL are preferable were reflect the higher shielding against gamma radiation [1,11]. In this study, host H glass sample with a nominal composition of B_2O_3- SiO_2- Al_2O_3- ZnO- Na_2O is singly and doubly doped with various concentrations of Tb^{3+} and 0.5%mol: Dy^{3+} ions (S1-S7) to be investigated by means of structural and radiation shielding properties. In fact, B_2O_3 and SiO_2 are commonly used as glass formers were the have high glass-forming ability (GFA) at lower melting points with good optical transparency in addition to their moderate rare-earth (RE) ion solubility. On the other hand, the Alkali oxide metal (Na_2O) reacts with the B2O3 former where part of the boron will modify in a bidirectional way $BO_3 \leftrightarrow BO_4$ in a complex manner. The aluminum oxide (Al_2O_3) addition improves the chemical durability, mechanical strength [12]. Furthermore, ZnO playing the role of imparting extension of UV optical transparency and enhanced glass forming region in oxide glasses [13]. These samples are characterized by XRD, Raman, FTIR and TGA/DSC analysis. Also, the radiation shielding is investigated theoretically through the evaluation of the shielding parameters mentioned above by using XCOM, WINXCOM and Phy-X [14,15] online programs as well as other relevant equations.

2. Experimental

Glass samples named as (H, S1-S7) were prepared by using a melt quenching technique with deferent concentration with the following composition

$$(60-x-y) \ B_2O_3\text{-}10 \ SiO_2\text{-}5 \ Al_2O_3\text{-}15 \ ZnO\text{-}10 \ Na_2O -x \ Dy_2O_3\text{-}y \ Tb_4O_7 \qquad (1)$$

where (x = 0.5) for all the glasses and x=0 for glass H and S2 while (y= 0, 0, 0.5,0.1, 0.25, 0.5, 0.75, 1.0) (mol %) for glasses (H, S1-S7), respectively. Each glass sample has 15g weight batches prepared and mixed before melting within a temperature of 975 °C for 30 minutes. Table 1 shows the glasses concentrations in mol% as well as their density, according to Archimedes' principle. The obtained glasses were transparent and bubble-free, having 3–4 cm diameter and ~0.3 cm thickness. The samples are annealed at 300 °C for 5 hours to eliminate the thermal stress, and then the samples were left to be cooled to the room temperature. Regarding the X-ray diffraction, structural and thermal analysis of the glasses (FTIR, Raman, TGA, and DSC), the equipment and measured parameters were used are reported in our earlier publication [16-18]. In brief, the XRD profiles were measured using Ital Structure APD 2000 diffractometer with an applied voltage of 40 kV and

20 mA anode current. Over the 250–4000 cm^{-1} range, the ATR-FTIR spectra of the glass were measured by a Perkin Elmer Spectrum 100 FTIR spectrometer with a resolution of ~4 cm^{-1}. The WITec alpha 300R Confocal Raman system is employed to obtain the Raman profiles of the samples. Thermo-gravimetric analysis (TGA) and differential scanning calorimetry (DSC) measurements were performed with a Mettler Toledo TGA/DSC 1 HT Integrated Thermal Gravimetric Analyzer and a flow rate of 50 mL/min.

Furthermore, some radiation shielding parameters pertaining to these glasses such as mass attenuation coefficient (μ/ρ), half-value layer (HVL), mean free path (MFP), have been evaluated with a gamma energy range of (0.015-15) MeV by using the suitable equations, XCOM, WINXCOM, and Phy-X programs.

Table 1
Glass composition in mol% and density (g cm^{-3})

Glass	B_2O_3	SiO_2	Al_2O_3	ZnO	Na_2O	Dy_2O_3	Tb_4O_7	Density
H	60	10	5	15	10	0	0	3.061
S1	59.5	10	5	15	10	0.5	0	3.100
S2	59.5	10	5	15	10	0	0.5	3.097
S3	59.4	10	5	15	10	0.5	0.1	3.107
S4	59.25	10	5	15	10	0.5	0.25	3.118
S5	59	10	5	15	10	0.5	0.5	3.136
S6	58.75	10	5	15	10	0.5	0.75	3.154
S7	58.5	10	5	15	10	0.5	1	3.173

3. Results and Discussion

3.1 Structural Properties

Figure 1 shows the XRD pattern of all the prepared samples were there are no sharp diffraction peaks are identified except the two diffuse bands at 20°- 50° range. So, one can confirm that the synthesized glasses are without any crystallization network. To identify the structure matrix network of the synthesized glasses, FTIR measurements spectra were recorded at a wavenumber of 400–4000 cm^{-1} and presented in Figure 2(a) (375-1500 cm^{-1}) and (b) (1500–4000 cm^{-1}). However, the IR vibrations of the borate-based glasses can be identified in (450–2000 cm^{-1}) region. Further, from Figure 2(a), it's clear that the bands at 435, 682, 894, 1058, 1226 and 1350 nm are asymmetric and broad due to the vibrational states degeneracy as well as the amorphous structure scattering of the glasses [19,20]. Further, one can observe that there is no deviation in the IR spectra of the samples, with the singly or doubly doped with Dy^{3+} or Tb^{3+} ions concentration (S1- S7). In Figure 2(b), the shallow oscillations can be observed which is related to glass interference [20].

Raman spectra in the range of (0-1600 cm^{-1}) can be shown for all the synthesized samples in Figure 3. The boson frequency region which is considered as a low-frequency region can be usually assigned around (100-180) cm^{-1} which belongs to BO_3 and BO_4 vibrational modes due to alkali/alkaline borates [18,21]. The Boson band of the glasses can be identified which is changed a little bit with the increment of Tb^{3+} ion content from 0.1 to 1.0 mol% (S3-S7). These changes belong to the induction of Tb^{3+} ions in the glass structure by means of incorporation of RE^{3+} at non-bridging anion bond sites were influence the values of the Boson peak [21]. For S3-S7 samples, the Raman band at 240 cm^{-1} identifies Metal–Oxygen (M–O) rotational and vibrational modes [18]. The bending vibration of Zn-O in ZnO_4 can be identified at 400-840 cm^{-1} bands region [22]. Also, these bands are due to the symmetric breathing vibrations of pentaborate groups and metaborate rings [23]. Bands at 852-1176 cm^{-1} belong to numerous functional groups of B_2O_3 such as symmetric breathing vibrations of a ring containing BO_3 units replaced by BO_4 tetrahedral, bending vibrations

of B-O-B bridges in metaborate groups of BO_3 units, B-O-B and B-O vibrational modes in orthoborate groups of BO_3 units and B-O bond stretching in BO_4 groups [18,24,25]. The Raman bands at 1200–1581 cm^{-1} corresponds to stretching vibrations due to the B-O bonds of pyroborate groups, vibrations bonds related to the BO_2O^- triangles linked with BO units, and B-O stretching vibrations including nonbridging oxygen (NBO) and being involved in the boron-oxygen network [18].
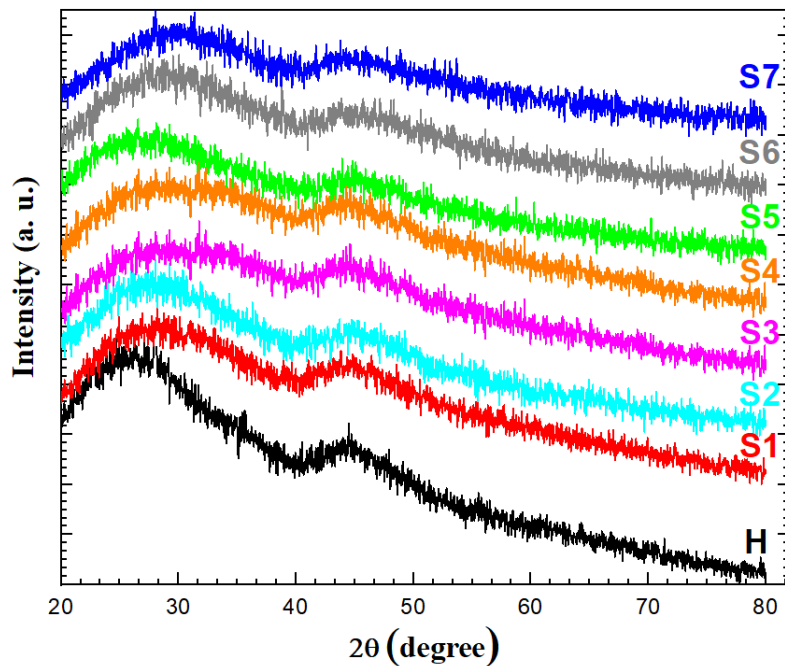
Fig. 1. XRD spectra of all the synthesized glasses
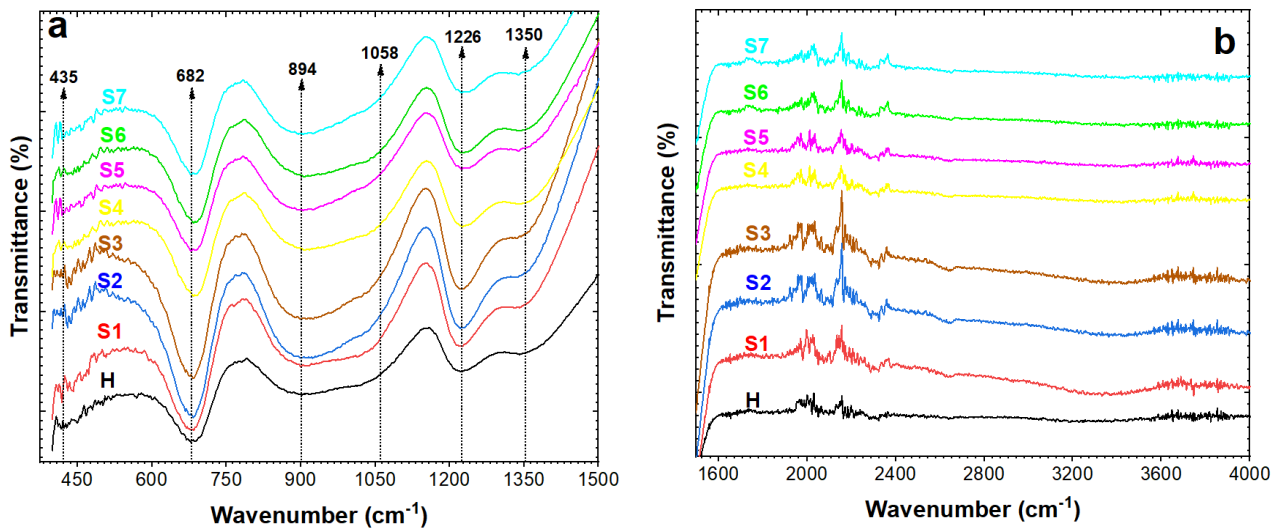
Fig. 2. ATR-FTIR spectra for all the synthesized glasses in the (a) 375-1500 cm^{-1} and (b) 1500–4000 cm^{-1} wavenumber region
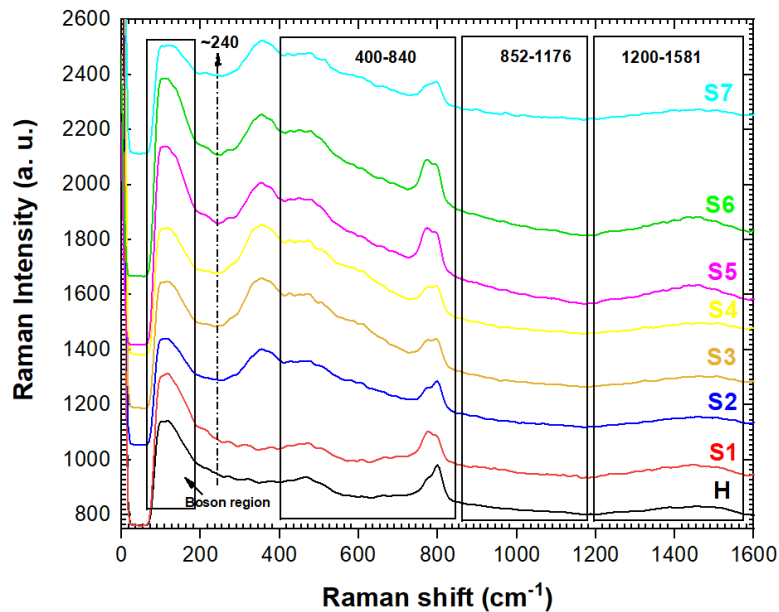
Fig. 3. Raman spectra for all glasses in the range of 0 –1600 cm^{-1}

3.2 Thermal Properties

TGA and DSC experiments were performed to investigate the thermal properties of the prepared samples as can be shown in Figure 4(a) and (b), respectively. In Figure 4(a), it's clear that there is a neglected weight loss below 100 °C which belongs to the evaporation of the residual water on the glass powder surface. During the heating treatment at temperature of 25–1000 °C, the identified weight losses of the samples (in %) are 1.4%, 1.6%, 0.3%, 0.9%, 1.0%, 1.3%, and 1.4%, for S1, S2, S3, S4, S5, S6 and S7 glasses. These values indicate the good stability of the glasses at a higher temperature. Figure 4(b) shows the DSC profile of the prepared samples. The crystallization temperature (T_c), crystallization onset temperature (T_x) and transition temperature (T_g) values for all the synthesized glasses are listed in the Table 2. The small endothermic peaks as shown in the figure as well as the broad exothermic peaks due to the slow crystallization process [18,26] which reflect the stability of all samples. Also, it's clear that the T_g temperature increase as the Tb^{3+} concentration increases. Further, the deference $\Delta T = (T_x - T_g)$ °C was calculated and found to be at value >100 °C which gives the prepared glasses good merit of stability for deferent applications [2].
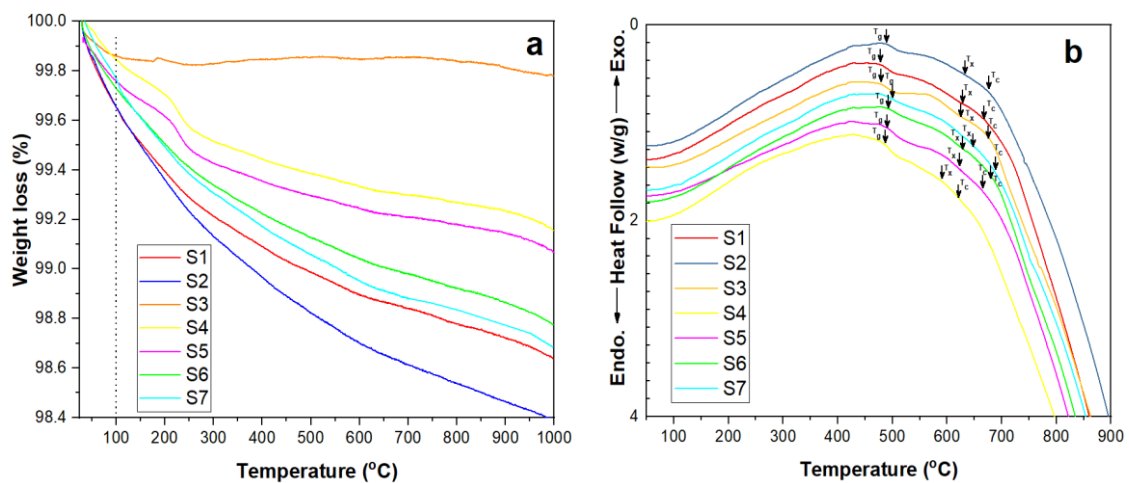
Fig. 4. (a) Thermo-gravimetric analysis (TGA) and (b) differential scanning calorimetry (DSC) profiles for the synthesized glasses

Table 2
Thermal properties of the glasses

Glass code	T_g (±0.5°C)	T_x (±0.5°C)	T_c (±0.5°C)	Glass Stability $\Delta T=(T_x-T_g)$ °C
S1	480	629	669	149
S2	476	634	676	158
S3	479	622	672	143
S4	486	593	620	107
S5	490	622	666	132
S6	492	627	679	135
S7	483	647	688	152

3.3 Radiation Shielding Parameters

The mass attenuation coefficient parameter (μ/ρ cm^2/g) which is related to the interaction) of photons with the shielding material is very important to qualify the glass samples. Normally, this parameter can be calculated through deferent software such as XCOM, WinXCOM, MCNPX Monte Carlo as well as phy-x program [15]. Half-Value-Layer (HVL) and Mean-Free-Path (MFP) values can be evaluated from this parameter. Theoretical values of the μ/ρ can be shown in Figure 5 for the synthesized samples and their changes with various energies as well as Tb^{3+} concentrations.
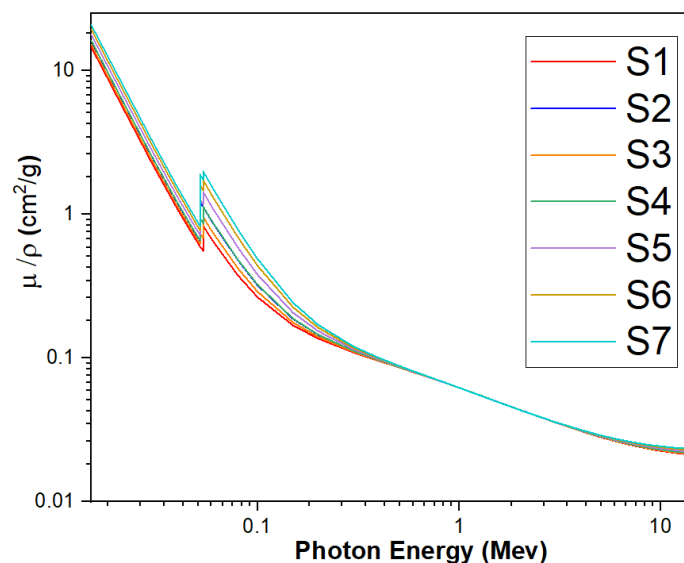
Fig. 5. Mass attenuation coefficients for all glasses

From Figure 5 one can observe that the μ/ρ values are increased to the Tb^{3+} increment while decrease if the photon energy increase. Further, the K-absorption edge made the sharp peak of the glass patterns to fall in the low region of energy precisely in the order of 31.18 keV - 37.44 keV [22, 27]. However, it's clear that S7 glass has the maximum value which confirms that the increment of Tb^{3+} ion makes the prepared glasses have better shielding properties. Another important parameter that reflects the properties of the prepared samples is the effective atomic number (Z$_{eff}$) and is usually computed through the following equation [28,29]

$$Z_{eff} = \frac{\sum_i f_i A_i \left(\frac{\mu}{\rho}\right)_i}{\sum_j f_j \frac{A_j}{z_j} \left(\frac{\mu}{\rho}\right)_j} \qquad (2)$$

where z_j is the atomic number, f_i is the fractional abundance of the element "i" and A_i is the atomic weight. In Figure 6, the Z_{eff} profiles of the synthesized glasses can be shown with a photon energy range of (0.015 MeV - 15 MeV). one can observe the significant changes in Z_{eff} values due to the interaction process of photons like photoelectric absorption, pair production and Compton scattering. The sudden jump of the sample profiles in the same figure at 0.06 MeV is pertaining to K-edge absorption for the heavy metal. At the same time, the Z_{eff} reduced strongly with energy of 0.06 MeV to 0.3 MeV due to the photoelectric process [22]. According to the sample profiles in this figure increment of Z_{eff} values are due to the increase in Tb^{3+} content where S7 sample has the highest value. This increment indeed leads to the enhancement of the radiation shielding performance. Upon the mass attenuation coefficient, Half-Value-Layer (HVL) and Mean-Free-Path (MFP) values of the synthesized samples can be calculated according to the following equations [30]

$$HVL = \frac{0.693}{\mu} \qquad (3)$$

$$MFP = \frac{1}{\mu} \qquad (4)$$

where μ is the linear attenuation coefficient and equal to (μ/ρ * density) of the glasses.
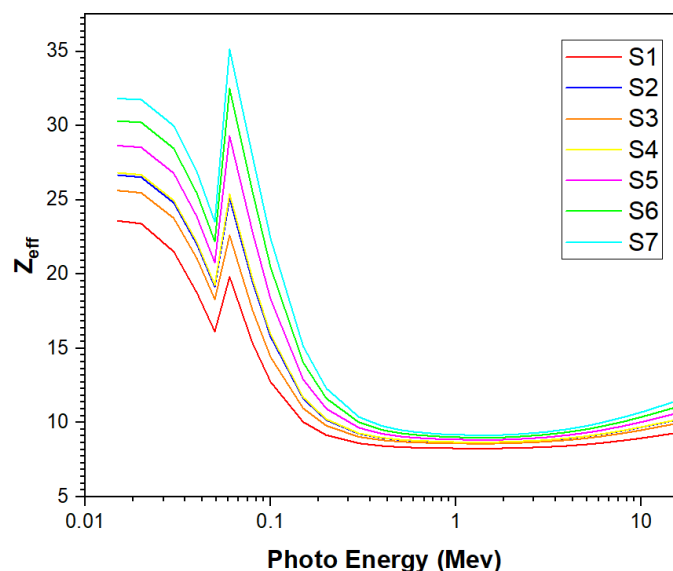
Fig. 6. Effective atomic number for all the prepared glasses

It is clear from Figure 7 and Figure 8 and their inset figures, the MFP as well as HVL have minimum values at low energy regions (E < 0.05 MeV) and almost they have the same values. But in the energy region of (0.05-0.34 MeV), the values of HVL are changing in the order of 136×10^{-3}- 2.04

cm while the MFP values are in the range of 196×10^{-3}- 3.02 cm. However, from the inset figures in Figure 7 and 8, it's clear that the increment of Tb^{3+} concentration causes the decrease of the HVL and MFP quantity. At the same time, the glass sample S7 (1.0 mol%: Tb^{3+}) has the lowest values. This phenomenon occurs due to the increment of samples density as well as their μ/ρ value. Additionally, MFP findings are compared with other reported works such as lead zinc phosphate glass GS1 [31], zinc oxide soda-lime silica glass G1 [32], and ordinary concrete [33] as presented in Table 3. A glance at this table, particularly at the energy range of (0.06-5 MeV), it is clear that the MFP findings of the prepared glasses have lower values than other mentioned glasses were they considered as a benchmark against this study which proves that the prepared glasses possess better shielding performance. So, depending on these findings, one can suggest aforementioned samples as a potential glass to be employed for radiation shielding applications.
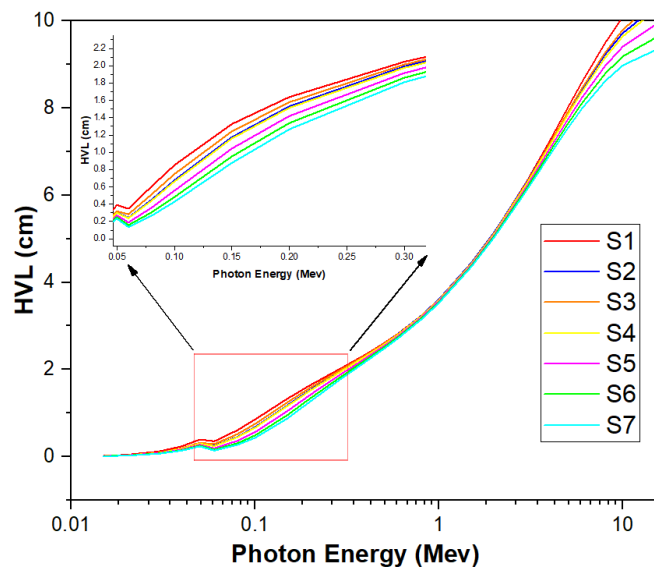
Fig. 7. HVL as a function of energy for all glass samples
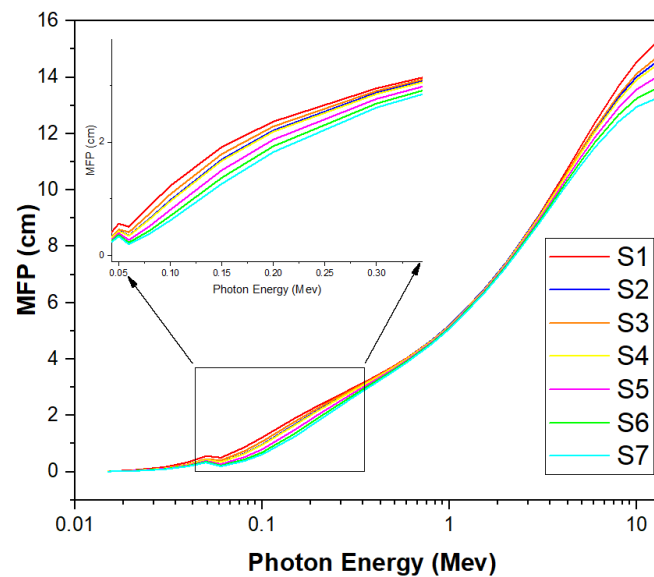
Fig. 8. MFP as a function of energy for all glass samples

Table 3
Comparison of Mean Free Path, MFP (cm) between prepared glasses and other works

Energy (MeV)	S1	S2	S3	S4	S5	S6	S7	[31]	[32]	[33]
0.015	0.02629	0.01918	0.02017	0.01887	0.01708	0.01565	0.01446	0.00769	0.06321	0.05302
0.02	0.0571	0.04162	0.04381	0.04094	0.037	0.03384	0.03125	0.01687	0.14545	0.12238
0.03	0.16725	0.12321	0.12974	0.12115	0.1094	0.09999	0.09226	0.05218	0.4412	0.37588
0.04	0.34173	0.25755	0.27076	0.25334	0.22938	0.21011	0.1942	0.11632	0.86564	0.72575
0.05	0.56193	0.43681	0.4576	0.42995	0.39155	0.36033	0.33433	0.21316	1.31107	1.12321
0.06	0.50541	0.35325	0.41083	0.34506	0.27392	0.22832	0.19653	0.3416	1.70062	1.48542
0.08	0.87141	0.64981	0.73846	0.6356	0.51845	0.43989	0.38343	0.66779	2.25672	2.02324
0.1	1.22908	0.97548	1.08156	0.95654	0.80548	0.69857	0.61872	1.02516	2.60681	2.36877
0.15	1.91611	1.69629	1.7938	1.67198	1.50602	1.37376	1.26548	2.24517	3.47542	3.20723
0.2	2.36461	2.20973	2.2789	2.18472	2.04739	1.92957	1.82682	2.83315	4.03726	3.73178
0.3	2.95178	2.87649	2.90738	2.85135	2.7648	2.68528	2.61123	3.2465	4.5177	4.17753
0.4	3.38081	3.34176	3.35423	3.31573	3.255	3.19755	3.14226	3.59037	4.95082	4.57859
0.5	3.74336	3.72332	3.72572	3.69593	3.64846	3.6028	3.55791	3.90001	5.3544	4.95203
0.6	4.07047	4.06192	4.05795	4.03295	3.9929	3.95393	3.91497	4.45769	6.09645	5.6386
0.8	4.65977	4.66469	4.65284	4.63248	4.59965	4.5672	4.53396	4.96616	6.78085	6.2717
1	5.19521	5.20843	5.1914	5.17299	5.14321	5.11346	5.08247	7.01496	9.65029	8.91965
1.5	6.39082	6.41239	6.3883	6.36931	6.33852	6.30744	6.27454	8.43827	11.85684	10.93974
2	7.41309	7.42878	7.40337	7.37871	7.33876	7.29873	7.25678	9.45539	13.60867	12.53148
3	9.10505	9.08192	9.06336	9.01963	8.94925	8.88	8.80961	10.18669	15.0215	13.80408
4	10.44708	10.36358	10.35908	10.29103	10.18214	10.07649	9.97132	10.7145	16.16359	14.82286
5	11.52731	11.37158	11.38511	11.29042	11.13969	10.99495	10.85298	11.08885	17.08936	15.64201
6	12.40047	12.16775	12.20091	12.07927	11.88658	11.70306	11.52499	11.35431	17.84904	16.30818
8	13.69123	13.30293	13.37627	13.20299	12.93077	12.6748	12.43028	11.54131	18.47082	16.84767
10	14.55523	14.0235	14.13442	13.91521	13.5732	13.25474	12.9539	11.66638	18.98113	17.28623
15	15.70254	14.88774	15.07446	14.76704	14.29363	13.86031	13.45841	11.8403	20.49062	18.54699

4. Conclusions

Multicomponent of borosilicate glass samples (H, S1-S7) were prepared by using melt quenching process. From the XRD results the amorphous nature was confirmed for the prepared glasses. Multi-functional groups were confirmed from FTIR and Raman spectra findings. Thermal stability as well as the optical transparency of the synthesized glasses were proved. WINXCOM and XCOM online programs in addition to the other relevant equation were employed to evaluate the radiation shielding properties of the prepared glasses. Within energy range of (0.015-15 MeV), the μ/ρ and Z_{eff} values are increasing with the increment of Tb^{3+} ion concentration, while HVL and MFP values are decreasing. However, the S7 sample showed the optimum shielding performance compared to other samples upon the selected energy. Furthermore, from the point of comparison, it is clear that at the photon energy range of (0.06-5 MeV), the MFP findings of the prepared glasses have lower values than some other related works. So, upon these findings, one can indicate the enhancement of shielding capability of the synthesized glasses and suggesting them to be utilized as shielding materials against gamma-ray applications.

Acknowledgement

References

[1] Elmahroug, Y., B. Tellili, and C. Souga. "Determination of shielding parameters for different types of resins." *Annals of Nuclear Energy* 63 (2014): 619-623.
https://doi.org/10.1016/j.anucene.2013.09.007

[2] Lakshminarayana, G., M. I. Sayyed, S. O. Baki, A. Lira, M. G. Dong, Kh A. Bashar, I. V. Kityk, and M. A. Mahdi. "Borotellurite glasses for gamma-ray shielding: an exploration of photon attenuation coefficients and structural and thermal properties." *Journal of Electronic Materials* 48, no. 2 (2019): 930-941.
https://doi.org/10.1007/s11664-018-6810-8

[3] Bashar, Kh A., W. L. Fong, Kh A. Haider, S. O. Baki, M. H. M. Zaid, and M. A. Mahdi. "Optical studies on Tb^{3+}: Dy^{3+} singly and doubly doped Borosilicate glasses for white light and solid state lighting applications." *Journal of Non-Crystalline Solids* 534 (2020): 119943.
https://doi.org/10.1016/j.jnoncrysol.2020.119943

[4] Kaur, Updesh, J. K. Sharma, Parjit S. Singh, and Tejbir Singh. "Comparative studies of different concretes on the basis of some photon interaction parameters." *Applied Radiation and Isotopes* 70, no. 1 (2012): 233-240.
https://doi.org/10.1016/j.apradiso.2011.07.011

[5] Kaur, Sandeep, and K. J. Singh. "Investigation of lead borate glasses doped with aluminium oxide as gamma ray shielding materials." *Annals of Nuclear Energy* 63 (2014): 350-354.
https://doi.org/10.1016/j.anucene.2013.08.012

[6] Sayyed, M. I. "Half value layer, mean free path and exposure buildup factor for tellurite glasses with different oxide compositions." *Journal of Alloys and Compounds* 695 (2017): 3191-3197.
https://doi.org/10.1016/j.jallcom.2016.11.318

[7] Chanthima, N., J. Kaewkhao, P. Limkitjaroenporn, S. Tuscharoen, S. Kothan, M. Tungjai, S. Kaewjaeng, S. Sarachai, and P. Limsuwan. "Development of BaO–ZnO–B_2O_3 glasses as a radiation shielding material." *Radiation Physics and Chemistry* 137 (2017): 72-77.
https://doi.org/10.1016/j.radphyschem.2016.03.015

[8] Issa, Shams AM, and A. M. A. Mostafa. "Effect of Bi_2O_3 in borate-tellurite-silicate glass system for development of gamma-rays shielding materials." *Journal of Alloys and Compounds* 695 (2017): 302-310.
https://doi.org/10.1016/j.jallcom.2016.10.207

[9] Sayyed, M. I., and H. Elhouichet. "Variation of energy absorption and exposure buildup factors with incident photon energy and penetration depth for boro-tellurite (B_2O_3-TeO_2) glasses." *Radiation physics and chemistry* 130 (2017): 335-342.
https://doi.org/10.1016/j.radphyschem.2016.09.019

[10] Bagheri, Reza, Alireza Khorrami Moghaddam, and Hassan Yousefnia. "Gamma ray shielding study of barium–bismuth–borosilicate glasses as transparent shielding materials using MCNP-4C code, XCOM program, and available experimental data." *Nuclear Engineering and Technology* 49, no. 1 (2017): 216-223. https://doi.org/10.1016/j.net.2016.08.013

[11] Sayyed, M. I. "Investigation of shielding parameters for smart polymers." *Chinese journal of physics* 54, no. 3 (2016): 408-415. https://doi.org/10.1016/j.cjph.2016.05.002

[12] Berger, M. J., J. H. Hubbell, S. M. Seltzer, J. Chang, J. S. Coursey, R. Sukumar, D. S. Zucker, and K. Olsen. "XCOM: photon cross sections database NIST Stand." *Ref. Database 8 XGAM* (1998): 87-93.

[13] Şakar, Erdem, Özgür Fırat Özpolat, Bünyamin Alım, M. I. Sayyed, and Murat Kurudirek. "Phy-X/PSD: development of a user friendly online software for calculation of parameters relevant to radiation shielding and dosimetry." *Radiation Physics and Chemistry* 166 (2020): 108496. https://doi.org/10.1016/j.radphyschem.2019.108496

[14] Lakshminarayana, G., Kh A. Bashar, S. O. Baki, A. Lira, U. Caldiño, A. N. Meza-Rocha, C. Falcony, E. Camarillo, I. V. Kityk, and M. A. Mahdi. "Er^{3+}/Dy^{3+} codoped B_2O_3-TeO_2-PbO-ZnO-Li_2O-Na_2O glasses: Optical absorption and fluorescence features study for visible and near-infrared fiber laser applications." *Journal of Non-Crystalline Solids* 503 (2019): 366-381. https://doi.org/10.1016/j.jnoncrysol.2018.10.025

[15] Mohammed, Al-BFA, G. Lakshminarayana, S. O. Baki, Kh A. Bashar, I. V. Kityk, and M. A. Mahdi. "Optical and dielectric studies for Tb^{3+}/Sm^{3+} co-doped borate glasses for solid-state lighting applications." *Optical Materials* 86 (2018): 387-393. https://doi.org/10.1016/j.optmat.2018.10.033

[16] Bashar, Kh A., G. Lakshminarayana, S. O. Baki, Al-BFA Mohammed, U. Caldiño, A. N. Meza-Rocha, Vijay Singh, I. V. Kityk, and M. A. Mahdi. "Tunable white-light emission from Pr^{3+}/Dy^{3+} co-doped B_2O_3-TeO_2 PbO-ZnO Li_2O-Na_2O glasses." *Optical Materials* 88 (2019): 558-569. https://doi.org/10.1016/j.optmat.2018.12.028

[17] Edukondalu, A., B. Kavitha, M. A. Samee, Shaik Kareem Ahmmed, Syed Rahman, and K. Siva Kumar. "Mixed alkali tungsten borate glasses–Optical and structural properties." *Journal of alloys and compounds* 552 (2013): 157-165. https://doi.org/10.1016/j.jallcom.2012.10.010

[18] Lakshminarayana, G., S. O. Baki, A. Lira, I. V. Kityk, U. Caldiño, Kawa M. Kaky, and M. A. Mahdi. "Structural, thermal and optical investigations of Dy^{3+}-doped B_2O_3–WO_3–ZnO–Li_2O–Na_2O glasses for warm white light emitting applications." *Journal of Luminescence* 186 (2017): 283-300. https://doi.org/10.1016/j.jlumin.2017.02.049

[19] Lakshminarayana, G., S. O. Baki, A. Lira, U. Caldiño, A. N. Meza-Rocha, I. V. Kityk, A. F. Abas, M. T. Alresheedi, and M. A. Mahdi. "Effect of alkali/mixed alkali metal ions on the thermal and spectral characteristics of Dy^{3+}: B_2O_3-PbO-Al_2O_3-ZnO glasses." *Journal of Non-Crystalline Solids* 481 (2018): 191-201. https://doi.org/10.1016/j.jnoncrysol.2017.10.047

[20] Sayyed, M. I., and G. Lakshminarayana. "Structural, thermal, optical features and shielding parameters investigations of optical glasses for gamma radiation shielding and defense applications." *Journal of Non-Crystalline Solids* 487 (2018): 53-59. https://doi.org/10.1016/j.jnoncrysol.2018.02.014

[21] Yadav, Avadhesh Kumar, and Prabhakar Singh. "A review of the structures of oxide glasses by Raman spectroscopy." *RSC advances* 5, no. 83 (2015): 67583-67609. https://doi.org/10.1039/C5RA13043C

[22] Osipov, Armenak A., and Leyla M. Osipova. "Raman scattering study of barium borate glasses and melts." *Journal of Physics and Chemistry of Solids* 74, no. 7 (2013): 971-978. https://doi.org/10.1016/j.jpcs.2013.02.014

[23] He, Feng, Zijun He, Junlin Xie, and Yuhui Li. "IR and Raman spectra properties of Bi_2O_3-ZnO-B_2O_3-BaO quaternary glass system." *American Journal of Analytical Chemistry* 5, no. 16 (2014): 1142. https://doi.org/10.4236/ajac.2014.516121

[24] Hamza, A. M., M. K. Halimah, F. D. Muhammad, K. T. Chan, A. Usman, M. F. Faznny, I. Zaitizila, and R. A. Tafida. "Structural, optical and thermal properties of Er^{3+}-Ag codoped bio-silicate borotellurite glass." *Results in Physics* 14 (2019): 102457. https://doi.org/10.1016/j.rinp.2019.102457

[25] Singh, Kulwant, Harvinder Singh, Vishal Sharma, Rohila Nathuram, Atul Khanna, Rajesh Kumar, Surjit Singh Bhatti, and Hari Singh Sahota. "Gamma-ray attenuation coefficients in bismuth borate glasses." *Nuclear instruments and methods in physics research section B: Beam Interactions with Materials and Atoms* 194, no. 1 (2002): 1-6.

Penerbit
Akademia Baru

https://doi.org/10.1016/S0168-583X(02)00498-6

[26] Sayyed, M. I., Shams AM Issa, and Sayed H. Auda. "Assessment of radio-protective properties of some anti-inflammatory drugs." *Progress in Nuclear Energy* 100 (2017): 297-308.
https://doi.org/10.1016/j.pnucene.2017.07.003

[27] Kurudirek, Murat. "Effective atomic numbers and electron densities of some human tissues and dosimetric materials for mean energies of various radiation sources relevant to radiotherapy and medical applications." *Radiation Physics and Chemistry* 102 (2014): 139-146.
https://doi.org/10.1016/j.radphyschem.2014.04.033

[28] Zoulfakar, A. M., A. M. Abdel-Ghany, T. Z. Abou-Elnasr, A. G. Mostafa, S. M. Salem, and H. H. El-Bahnaswy. "Effect of antimony-oxide on the shielding properties of some sodium-boro-silicate glasses." *Applied Radiation and Isotopes* 127 (2017): 269-274.
https://doi.org/10.1016/j.apradiso.2017.05.007

[29] Khanna, Atul, Amanpreet Saini, Banghao Chen, Fernando González, and Carmen Pesquera. "Structural study of bismuth borosilicate, aluminoborate and aluminoborosilicate glasses by 11B and 27Al MAS NMR spectroscopy and thermal analysis." *Journal of non-crystalline solids* 373 (2013): 34-41.
https://doi.org/10.1016/j.jnoncrysol.2013.04.020

[30] Colak, S. Cetinkaya, I. Akyuz, and F. Atay. "On the dual role of ZnO in zinc-borate glasses." *Journal of Non-Crystalline Solids* 432 (2016): 406-412.
https://doi.org/10.1016/j.jnoncrysol.2015.10.040

[31] El-Bashir, B. O., M. I. Sayyed, M. H. M. Zaid, and K. A. Matori. "Comprehensive study on physical, elastic and shielding properties of ternary $BaO-Bi_2O_3-P_2O_5$ glasses as a potent radiation shielding material." *Journal of Non-Crystalline Solids* 468 (2017): 92-99.
https://doi.org/10.1016/j.jnoncrysol.2017.04.031

[32] Sayyed, M. I., Y. Elmahroug, B. O. Elbashir, and Shams AM Issa. "Gamma-ray shielding properties of zinc oxide soda lime silica glasses." *Journal of Materials Science: Materials in Electronics* 28, no. 5 (2017): 4064-4074.
https://doi.org/10.1007/s10854-016-6022-z

[33] Bashter, I. I. "Calculation of radiation attenuation coefficients for shielding concretes." *Annals of nuclear Energy* 24, no. 17 (1997): 1389-1401.
https://doi.org/10.1016/S0306-4549(97)00003-0